


Altered Structure and Intrinsic Functional Connectivity in Post-stroke Aphasia

Mi Yang^{1,2} · Pu Yang¹ · Yun-Shuang Fan¹ · Jiao Li¹ · Dezhong Yao¹ · Wei Liao¹ ·
Huafu Chen¹ 

Received: 17 January 2017 / Accepted: 13 September 2017 / Published online: 18 September 2017
© Springer Science+Business Media, LLC 2017

Abstract Previous studies have demonstrated that alterations of gray matter exist in post-stroke aphasia (PSA) patients. However, so far, few studies combined structural alterations of gray matter volume (GMV) and intrinsic functional connectivity (iFC) imbalances of resting-state functional MRI to investigate the mechanism underlying PSA. The present study investigated specific regions with GMV abnormality in patients with PSA ($n = 17$) and age- and sex-matched healthy controls (HCs, $n = 20$) using voxel-based morphometry. In addition, we examined whether there is a link between abnormal gray matter and altered iFC. Furthermore, we explored the correlations between abnormal iFC and clinical scores in aphasic patients. We found significantly increased GMV in the right superior temporal gyrus, right inferior parietal lobule (IPL)/supramarginal gyrus (SMG), and left middle occipital gyrus. Decreased GMV was found in the right caudate gyrus, bilateral thalami in PSA patients. Patients showed increased remote interregional FC between the right IPL/SMG and right precuneus, right angular gyrus, right superior occipital gyrus; while reduced FC in the right caudate gyrus and supplementary motor area, dorsolateral superior frontal gyrus. Moreover, iFC strength between the left middle occipital gyrus and

the left orbital middle frontal gyrus was positively correlated with the performance quotient. We suggest that GMV abnormality contributes to interregional FC in PSA. These results may provide useful information to understand the pathogenesis of post-stroke aphasia.

Keywords Gray matter volume · Intrinsic functional connectivity · Post-stroke aphasia · Resting-state

Abbreviations

ABC	Aphasia battery of Chinese
AQ	Aphasia quotient
CQ	Cortical quotient
FD	Frame-wise displacement
fMRI	Functional magnetic resonance imaging
GMV	Gray matter volume
iFC	Intrinsic functional connectivity
PQ	Performance quotient
PSA	Post-stroke aphasia
VBM	Voxel-based morphometry

Introduction

Post-stroke aphasia (PSA) usually arising from left hemisphere lesions, causes significant cognitive impairment leading to substantial functional disability and high psychological distress (Berthier 2005). To further understand PSA, a number of studies on language architecture and that involved dynamic neurobiological mechanisms have been carried out (Ellis et al. 2012). However, the pathophysiology underlying PSA is still not entirely understood.

Patients with PAS usually have obvious lesions in both gray and white matter, which results in language deficits (Kochunov et al. 2007; Geva et al. 2012; Yang et al.

✉ Wei Liao
weiliao.wl@gmail.com

✉ Huafu Chen
chenhf@uestc.edu.cn

¹ Key Laboratory for NeuroInformation of Ministry of Education, Center for Information in BioMedicine, School of Life Science and Technology, University of Electronic Science and Technology of China, Chengdu 610054, People's Republic of China

² Department of Stomatology, the Fourth People's Hospital of Chengdu, Chengdu 610036, People's Republic of China

2017). A widely used morphological measurement in brain diseases is gray matter volume (GMV) (Ashburner and Friston 2000), which can be quantitatively calculated by voxel-based morphometry (VBM). Here, we used VBM to calculate the abnormalities of GMV to investigate altered brain structure in PSA patients. During spatial normalization of VBM, inaccurate tissue type classifications may occur as a result of the presence of lesions during the warping of individual brains to the standard template. To eliminate this influence, we masked out the lesions during the warping process, using a cost-function technique (Brett et al. 2001). This process requires the calculation of parameters accurately normalize individual lesioned brains to a common template without the potential influence of lesions. Studies trying to map post-stroke cognitive or motor symptoms to lesion locations have been available for a long time (Geva et al. 2012). It has been demonstrated that the alteration of gray matter is highly related to language comprehension deficits of aphasia patients (Ogar et al. 2011).

Intrinsic functional connectivity (iFC) is based on resting-state functional MRI (fMRI) and has been used to investigate the underlying mechanism of language processing in aphasia (van Hees et al. a, 2014b; Nair et al. 2015; Yang et al. 2016b). Alteration of iFC in the default-mode network (Wang et al. 2014) and the frontoparietal network (Zhu et al. 2014) in PSA patients has been confirmed in previous studies. Moreover, changes in regional brain activity and associated remote iFC patterns were also examined to enhance the understanding of the pathophysiological mechanisms of aphasia (Yang et al. 2016a).

It has been suggested that the brain structural connectivity may be the physical substrate of the brain functional connectivity (Greicius et al. 2009). The structural connections are highly predictive of and place constraints on functional interactions across the human brain (Honey et al. 2009). Moreover, the coupling of functional and structural connectivity has been found to increase with age (Hagmann et al. 2010) and to be disrupted in various disease-specific states (Liao et al. 2011a, b, 2017; Zhang et al. 2011; Ji et al. 2014; Long et al. 2017). Nevertheless, the relationship between structural changes and iFC in aphasia is still unclear, which is beneficial to further understand the pathophysiology underlying aphasia. Therefore, the combination of structural alteration and iFC is needed to simultaneously explored structural and functional brain abnormalities in PSA patients. In the present study, we performed an analysis by combining VBM and iFC to examine potential differences in the regional GMV and iFC between PSA patients and controls. Furthermore, we calculated the correlations between iFC strength and stroke-related clinical characteristics of the patients.

Materials and Methods

Subjects

Seventeen patients with PSA (all right-handed, six females and 11 males; aged, 53.53 ± 14.06 years) were recruited from Fuzhou Hospital. These patients had participated in one of our earlier studies (Yang et al. 2016a, b, 2017). Patients were recruited according to the following inclusion criteria: (i) first stroke occurred in the left hemisphere; (ii) age of >18 and <85 years; (iii) native Chinese speaker; (iv) aphasia persistent at day 1 post-stroke; and (v) right-handed. Participants were excluded if they fulfilled and of the following criteria: (i) any past or current neurological disorders or family history of hereditary neurological disorders; (ii) a history of head injury resulting in loss of consciousness; (iii) alcohol or substance abuse; (iv) claustrophobia; and (v) incompatible implants. Demographic and clinical characteristics for patients and age-, gender-, and education-matched HCs are listed in Tables 1 and 2 of our previous study (Yang et al. 2016a). The current study was approved by the local Ethics Committee of the Hospital of Fuzhou and was performed following the approved guidelines. All participants gave informed consent to participate in the investigation.

All patients received a comprehensive evaluation, including medical history and neurological examination, neuropsychological testing, and neuroimaging (Yang et al. 2016a). Aphasia was diagnosed based on the Aphasia Battery of Chinese (ABC), which is the Chinese standardized adaptation of the Western Aphasia Battery (Gao et al. 1992; Lu et al. 2013). The ABC provides an aphasia quotient (AQ), a performance quotient (PQ), and a cortical quotient (CQ) (Liu et al. 2015).

Table 1 Regions showing abnormal grey matter volume in patients

Brain regions	Brod-mann area	MNI (x, y, z)	Cluster size (voxels)	T value
Aphasia > HC				
R STG	22	(58, -46, 16)	1286	5.29
R IPL/SMG	42	(58, -48, 26)	496	5.29
L MOG	19	(-36, -66, 32)	282	4.49
Aphasia < HC				
R CAU	-	(16, 20, 8)	366	-5.40
R THA	-	(18, -20, 18)	276	-6.42
L THA	-	(-4, -10, 12)	156	-5.26

STG superior temporal gyrus, IPL inferior parietal lobule, SMG supramarginal gyrus, MOG middle occipital gyrus, CAU caudate gyrus, THA thalamus, L left, R right

x, y, z, coordinates of primary peak locations in the Montreal Neurological Institute (MNI) space; T value, statistical value of peak voxel showing GMV differences between the groups

Table 2 Intrinsic functional connectivity abnormalities in patients

Seed region	Connected regions	Brodmann area	MNI (x, y, z)	Cluster size (voxels)	T value
R CAU	L SFGdor	6	(- 18, 6, 69)	45	- 4.14
	L SMA	6	(- 6, 12, 63)	36	- 3.08
R IPL/SMG	R PCUN	-	(6, - 57, 42)	307	4.59
	R ANG	39	(48, - 51, 36)	201	4.82
	R SOG	7	(30, - 75, 42)	23	4.05
L MOG	L MFG	6	(- 39, 9, 54)	107	- 5.09
	L ORBinf	47	(- 45, 45, - 12)	69	- 3.92
	L ORBmid	47	(- 33, 45, - 3)	57	- 3.52
	R ANG	39	(42, - 57, 33)	106	- 3.62
	R IPL	39	(42, - 63, 45)	60	- 3.59
L THA	R CUN	-	(6, - 81, 39)	179	5.15
	R PCUN	7	(27, - 69, 39)	110	4.36
	L CUN	-	(- 6, 87, 36)	105	4.28
	R PreCG	6	(57, 0, 48)	104	3.89
	R PoCG	3	(57, - 12, 36)	72	3.88
R THA	R PCUN	-	(18, - 66, 21)	75	4.06
	R IPL	40	(42, - 57, 57)	20	3.52
	R SPG	7	(30, - 66, 54)	46	3.34

SFGdor superior frontal gyrus, dorsolateral, *SMA* supplementary motor area

x, y, z, coordinates of primary peak locations in the Montreal Neurological Institute (MNI) space; T value, statistical value of peak voxel showing FC differences between the groups

Data Acquisition

Imaging was performed using a 3.0T Siemens Vision Scanner (Erlangen, Germany). The following parameters were used for 3D T1 imaging: repetition time/echo time (TR/TE) = 2300/2.98 ms, matrix = 512 × 512, flip angle = 9°, voxel size = 0.5 × 0.5 × 1 mm³, 176 axial slices without interslice gap. Functional images were acquired from the same locations as the anatomical slices using an echo-planar imaging sequence with the following parameters: TR/TE = 2000/30 ms, matrix = 64 × 64, flip angle = 90°, interslice gap = 4.0 mm, voxel size = 3.8 × 3.8 × 4 mm³, and

slices = 31. For each participant, the fMRI scan lasted for 6 min, and 190 volumes were obtained.

Lesion Mapping

A radiologist (Y.L.) manually traced the outline of the lesion on individual 3D T1 images using MRIcron, thereby creating a lesion mask for each patient. The union of all individual lesion masks (after the spatial normalization process) was used to construct a group lesion mask for the patients (Fig. 1).

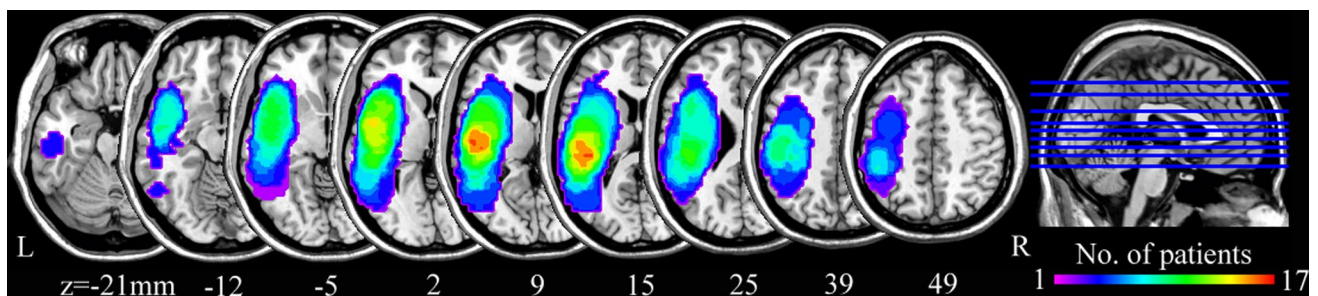


Fig. 1 Distribution of the lesion areas for all aphasic patients. The lesion area overlap across patients was rendered on the brain. Colors represent the number of patients with a lesion to a specific voxel.

Numbers below each axial map and sagittal map refer to the z-plane and x-plane coordinates of the MNI space, respectively. Letters L and R correspond to the left and right sides of the brain, respectively

Gray Matter Volume Analysis

The 3D T1 images were processed using a modified optimized VBM technique (SPM8, <http://www.fil.ion.ucl.ac.uk/spm>) (Ashburner and Friston 2000; Good et al. 2001). Moreover, we used a cost-function modification to remove the lesion area in 3D T1 images according to individual patient's lesion masks (Brett et al. 2001). After removal of the lesion, the 3D T1 images were normalized to the Montreal Neurological Institute (MNI) template using a 12-parameter affine transformation with nonlinear adjustments. The spatial transformation parameters were then applied to the 3D T1 volumes. The resultant normalized images were resampled to a $1 \times 1 \times 1 \text{ mm}^3$ voxel size and smoothed with an 8-mm full width half maximum Gaussian kernel. The images were averaged to produce a sample-specific whole brain template. Templates for gray matter, white matter, and cerebrospinal fluid were computed by segmentation (Ashburner and Friston 2000).

The second step in VBM processing involved the normalization of individual scans to the sample-specific template. After removal of the lesions, the 3D T1 images were segmented into gray matter, white matter, and cerebrospinal fluid components using information from the sample-specific tissue classification templates. Masking out the location of infarcts allowed for the calculation of tissue segmentation and normalization parameters devoid of potential tissue misclassification and normalization distortion induced by the presence of lesions. Individual lesion-adjusted normalized whole brain volumes were then segmented again into gray matter, white matter, and cerebrospinal fluid partitions using a Markov random field model (Cuadra et al. 2005) to improve tissue type classification. The segmented, normalized, and modulated individual lesion-adjusted brain segments were smoothed with an 8-mm full width half maximum Gaussian kernel. Application of the smoothing kernel compensates for inter-individual variability and conforms the data more closely to Gaussian random field theory, which provides corrected statistical inference.

Functional Image Preprocessing

Functional images were preprocessed using DPARSF (<http://www.restfmri.net>) (Chao-Gan and Yu-Feng 2010). The first ten functional volumes were discarded as signal equilibrium. We corrected the remaining images for temporal differences and head motion. No translation or rotation parameters in any given data set exceeded $\pm 1 \text{ mm}$ or $\pm 1^\circ$. Owing to the correlation between individual differences and motion-associated differences (Zeng et al. 2014), we also calculated individual mean frame-wise displacement (FD) by translation and rotation parameters of head motion based on the formula from a previous study (Power et al. 2012) and to evaluate

group differences. No difference was observed for mean FD between groups (Mann Whitney U-test, $P=0.12$). Spatial normalization of the functional images was performed using 3D T1-based transformation. We coregistered individual 3D T1 images to functional images. The 3D T1 images were segmented and normalized to MNI space by a 12-parameter nonlinear transformation. In addition, we used a cost-function modification to exclude the lesion area, avoiding bias during spatial normalization (Brett et al. 2001). This process has been implemented in SPM8 and was adopted in other brain imaging studies with lesions (Stebbins et al. 2008). These transformation parameters were applied to functional images. After spatial normalization, functional images were resampled at a voxel size of $3 \times 3 \times 3 \text{ mm}^3$. We then spatially smoothed the images with an 8 mm full-width half-maximum isotropic Gaussian kernel. Finally, we removed linear trends from the time courses and with temporal band-pass filtering (0.01–0.08 Hz).

Intrinsic Functional Connectivity (iFC) Analysis

Intrinsic functional connectivity analysis was performed using a temporal correlation approach (Fox et al. 2005). Regions showing significantly altered GMV were defined as a seed region for subsequent iFC analysis. The averaged time course was obtained from the seed region, and temporal correlation analysis was performed using a voxel-wise technique to generate the iFC map. In addition, six motion parameters, cerebrospinal fluid, and white matter signals were removed as nuisance variables to reduce the effects of head motion and non-neuronal fluctuations.

Statistical Analysis

To evaluate GMV differences between patients and HCs, we used two-sample t-tests on the lesion-adjusted MRI images using the SPM8 toolkit. Group comparison was applied within the patients' group masks to exclude the lesions in all patients. We included age, gender, education level, and individual whole brain GMV as covariates. The significance threshold was set to an AlphaSim corrected p value <0.005 and a minimum cluster size of 401 voxels. This process is based on the Monte Carlo simulation of calculating the probability of false positive detection by considering individual voxel probability thresholding and cluster size. We computed this number of voxels by the estimated smoothness with a statistical map (two-sample t-tests map) under the patients' group mask.

To compare iFC maps between group, we first used one-sample t-tests on iFC maps of PSA patients and HCs within the mask which excluded the lesions in all patients to create specific masks of PSA patients and HCs. We then added the specific mask of PSA patients to HCs'

specific mask to get the mask used for two-sample t-tests. Finally, two-sample t-tests were performed on iFC maps within the obtained mask to investigate iFC differences between patients and HCs. We included age, gender and education level as covariates. The significance threshold was set to an AlphaSim corrected p value < 0.005 and a minimum cluster size of voxels that depended on the size of iFC maps.

Finally, due to limited sample size, we used Spearman's rank correlation to determine whether the iFC strength was correlated with the clinical ABC scores in patients. We determined the mean z -value of FC strength as the FC value of each patient in the region of interest, which was the abnormal region in aphasic patients, according to the result of the two-sample t-test. We then computed Spearman's rank correlation coefficient among these FC values and the clinical ABC scores. Given that these analyses were exploratory, we used an uncorrected statistical significance level of $p < 0.05$.

Results

Demographics and Clinical Characteristics of Participants

Patients with PSA and HCs did not significantly differ in age (two-sample t-tests, $P = 0.98$), gender (χ^2 -test, $P = 0.90$), or years of education (Mann Whitney U-test, $P = 0.58$) (see Table 1 in (Yang et al. 2016a)). Stroke-related clinical characteristics of the patients were tested using the ABC (Gao et al. 1992; Lu et al. 2013). A manually drawn outline of the lesion on the T1 image of patients of PSA is shown in Fig. 1.

Gray Matter Volume Comparison

Compared with HCs, patients showed significantly increased GMV in the right superior temporal gyrus (STG), right inferior parietal lobule (IPL)/supramarginal gyrus (SMG), and left middle occipital gyrus (MOG); while showing decreased GMV in the right caudate (CAU), and in bilateral thalami (Table 1; Fig. 2).

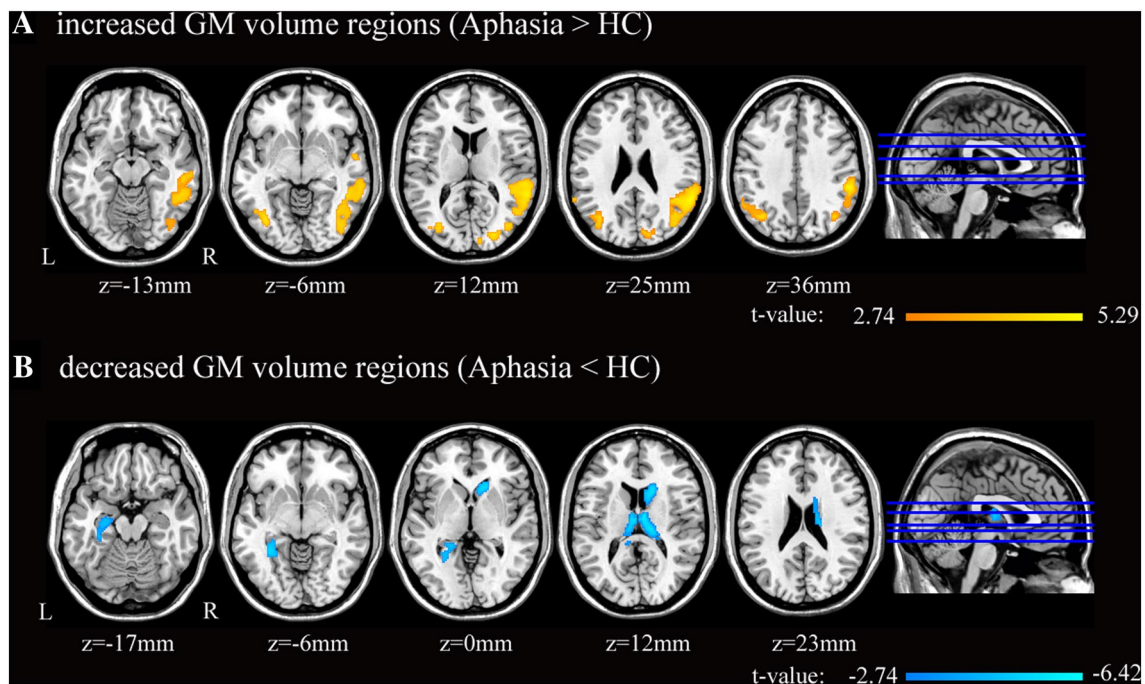


Fig. 2 Brain regions showing significant differences in GMV between patients with PSA and controls. **a** Warm colors indicate regions with increased GMV matter in aphasia. **b** Cold colors indicate regions with decreased GMV in aphasia. All comparisons were performed using two-sample t-tests (AlphaSim-corrected $P < 0.005$;

minimum cluster size of 401 voxels). Numbers below each axial map refer to the z -plane coordinates of the MNI space, respectively. Letters L and R correspond to the left and right sides of the brain, respectively

Intrinsic Functional Connectivity Comparison

The significant gray matter abnormalities detected between PSA patients and HCs were selected as the seed areas for FC analyses. (Table 2; Fig. 3).

When the seed area was located in the right CAU, PSA patients showed decreased iFC in the left dorsolateral superior frontal gyrus (SFGdor), and supplementary motor area (SMA) (AlphaSim corrected $p < 0.005$ and minimum cluster size of 62 voxels).

When taking the right IPL/SMG as seed area, PSA patients showed increased connectivity in the right precuneus (PCUN), angular gyrus (ANG), and superior occipital gyrus (SOG) (AlphaSim corrected $p < 0.005$ and minimum cluster size of 157 voxels).

When selecting the left MOG as the seed area, PSA patients showed decreased connectivity in the left middle frontal gyrus (MFG), inferior frontal gyrus, orbital part (ORBinf), middle frontal gyrus, orbital part (ORBmid) and right ANG, and IPL (AlphaSim corrected $p < 0.005$ and minimum cluster size of 116 voxels).

When taking the left thalamus as the seed area, PSA patients showed increased connectivity in the right PCUN, precentral gyrus (PreCG), postcentral gyrus (PoCG) and bilateral cuneus (AlphaSim corrected $p < 0.005$ and minimum cluster size of 130 voxels).

When selecting the right thalamus as the seed area, PSA patients showed increased connectivity in the right PCUN, IPL and superior parietal gyrus (SPG) (AlphaSim corrected $p < 0.005$ and minimum cluster size of 74 voxels).

However, when taking the right STG as the seed area, the result was no longer significant after AlphaSim correction.

Correlations Between iFC and Clinical Characteristics

We calculated the Spearman's rank correlation between altered interregional FC values and clinical characteristics of PSA patients. The iFC values between left MOG and left ORBmid were positively correlated with the performance quotient on the ABC ($Rho = 0.61$, $P = 0.01$) (Fig. 4). We found no other significant correlations between interregional iFC values and clinical characteristics.

Discussion

We examined abnormal GMV (by structural MRI) and iFC (by resting-state fMRI) alterations in patients with PSA. We found that patients showed significant GMV abnormalities in the right caudate, bilateral thalamus, right STG, right IPL/SMG and left MOG. To further investigate the influence of structural changes on functional circuits, seed-based resting-state iFC analysis was performed. Compared with

HCs, patients showed abnormal iFC when taking the right caudate, right IPL/SMG, left MOG, and bilateral thalamus as seed areas. These findings demonstrate that gray matter abnormalities were related to altered iFC in PSA patients.

Altered GMV in Right STG

A previous study found increased activation of the right STG during the recovery period of aphasic patients (Musso et al. 1999). These STG abnormalities can cause language difficulties as illustrated in the extreme cases of cortical deafness and receptive aphasia. These findings may suggest that, after left STG damage, gray matter of the right STG increases to compensate for contralateral language processing.

Altered GMV and iFC in Right IPL/SMG

The right SMG is considered to have an important role in phonological processing (Hartwigsen et al. 2010). A previous study showed that anterior and posterior SMG, opercular inferior frontal gyrus, and middle STG were causally related to single word production function (Sollmann et al. 2014). In addition, the right IPL is thought to play an important part in semantic processing (Chou et al. 2006a, b; Raposo et al. 2006). Thus, we suggest that increased right IPL/SMG volume was conducive to compensating phonological processing and word production. To further investigate the influence of increased right IPL/SMG volume to functional circuits, iFC analysis of right IPL/SMG was performed.

PSA patients exhibited increased iFC in the right PCUN, right ANG and right SOG. The anterior precuneus is implicated in self-referential processing, while the posterior region is associated with episodic memory and visuo-spatial imagery (Cavanna and Trimble 2006). The precuneus is also an essential hub of verbal politeness judgment (Ashizuka et al. 2015). The right ANG was found to be engaged in an assistive network in the case of extensive damage to left hemisphere language regions (Sims et al. 2016). A previous study showed that the greater GMV in the right superior occipital gyrus may reflect a neuroplastic change associated with brain reorganization to compensate for the left language lesion regions (Girbau-Massana et al. 2014). Therefore, we suggest that the increased connectivity in the right PCUN, ANG, and SOG may contribute to improving PSA patients' language processing, as well as cognitive impairment.

Altered GMV and iFC in Left MOG

The MOG is associated with word association and is part of the language network (Ghosh et al. 2010). In addition, occipitotemporal lesion disconnects visual processing in the occipital cortices from language processing in temporal and parietal regions of the left hemisphere, which indicates that

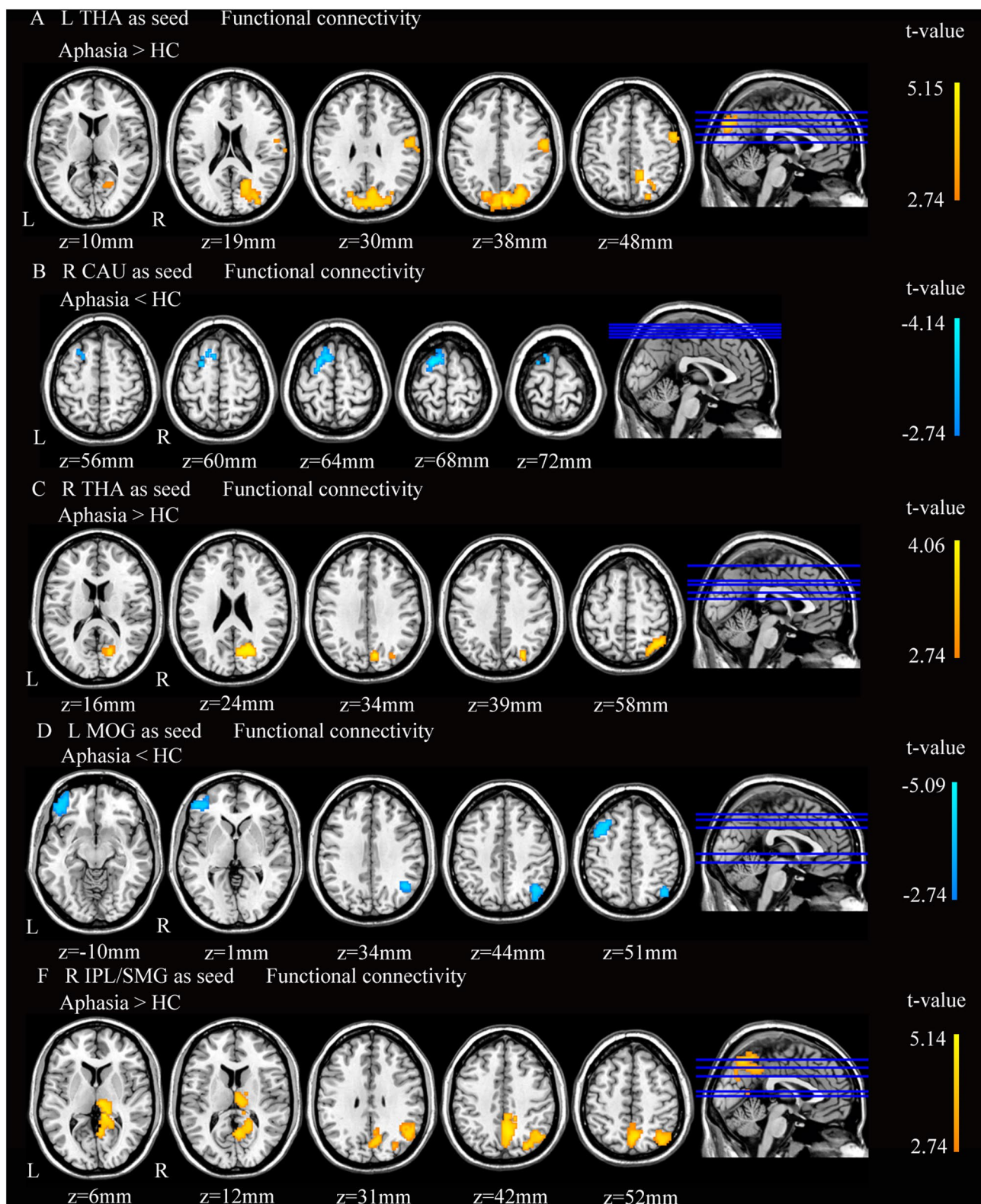


Fig. 3 Abnormalities of intrinsic functional connectivity in patients with PSA. Brain regions showing iFC differences between patients and controls by two-sample t-tests. Cold colors indicate regions with

decreased FC values in aphasia. Numbers below the axial slices refer to the z-plane coordinates of the MNI space. Letters L and R correspond to the left and right sides of the brain, respectively

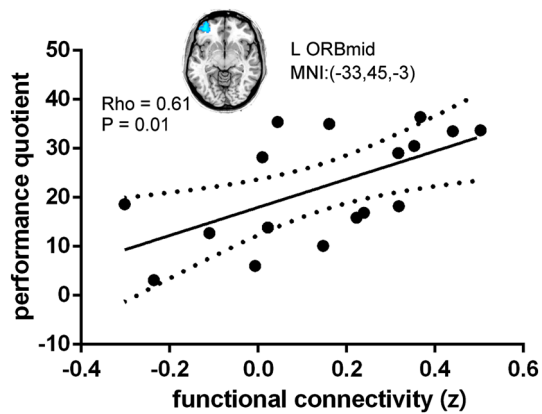


Fig. 4 Correlations between intrinsic functional connectivity strength and clinical scores in patients with PSA. The strength of iFC between the left middle occipital gyrus and the left middle frontal gyrus (orbital part) was positively correlated with the performance quotient in the aphasia battery of Chinese ($Rho=0.61$, $P=0.01$). Filled circles denote data points included in the correlation. Solid line and dashed lines represent the best-fit line and 95% confidence interval of Spearman's rank correlation, respectively

the occipital gyrus is related to pure alexia (Price and Devlin 2003). Patients with occipital lesions experienced difficulties in accessing words related to visual modality (Martensson et al. 2014). A previous study recommended aphasic patients to strengthen the function of left language-related regions (beyond the lesion areas) to compensate for language disability (Fridriksson et al. 2012). We calculated iFC maps using the left MOG as seed region to assess differences in the crosstalk among brain regions.

Patients with PSA exhibited decreased connectivity in the left MFG, ORBinf, ORBmid, right ANG, and IPL. The middle frontal gyrus is comparable to Broca's area in its ability to indicate hemispheric dominance for language using a measure of verbal fluency and may be an important measure in the clinical determination of language laterality for presurgical planning (Dong et al. 2016). Moreover, the left MFG plays a central part in language comprehension (Turken and Dronkers 2011). The orbital part of the left inferior frontal gyrus subserves the acquisition of linguistic knowledge in second language (Sakai et al. 2009). The orbital part of the inferior frontal gyrus and the mid-frontal cortex may also be related to language comprehension (Dronkers et al. 2004). Besides, the right ANG and IPL play a significant role in language processing (Chou et al. 2006a, b; Raposo et al. 2006; Sims et al. 2016). Therefore, we speculated that language disability in PSA patients led to decreased iFC connectivity in these regions. In addition, the FC values between left MOG and left ORBmid were positively correlated with PQ on the ABC in aphasic patients. Performance quotient is characterized by Drawing, Block design, numerical Calculation, and Reven's Colored Matrices Score (Charney 1981).

Our correlation analysis suggests that a low performance deficit is associated with low interregional functional connectivity activity between the left MOG and the left ORBmid. A previous study indicated that anomic aphasic patients who had left occipital lesions could not produce normal and detailed descriptions of both abstract and emotional words (Martensson et al. 2014). Moreover, semantic variant patients showed a strongly left-lateralized loss of hubs and a reduced nodal degree in occipital cortices (Agosta et al. 2014). Thus, we suggest that decreased connectivity between the left MOG and the left ORBmid contributes to cognitive impairment (e.g., poor performance abilities) of PSA patients.

Altered GMV and iFC in Right CAU

The responses of at least some neurons in the head of the CAU reflect the lexical semantic and phonological computations in a way similar to Broca's area (Abdullaev et al. 1998). Besides, the caudate networks are related to language, cognitive functions (e.g., executive functions and selective visual attention) (Radulescu et al. 2013). These findings may indicate that decreased GMV in the right CAU results in language and cognitive impairments in post-stroke aphasia.

The CAU and the SMA play a vital part in the word generation loop (Crosson et al. 2003). Therefore, we suggested that the damage in the word generation loop led to decreased connectivity in the left SMA. Neuroimaging studies of sentence comprehension showed low functional connectivity between caudate and frontal language/cognitive control regions in autism patients compared with controls (Just et al. 2004; Kana et al. 2006), which suggested that functional connectivity between the caudate and the SFGdor contributed to cognitive control impairment.

Altered GMV and iFC in Bilateral THA

The THA is related to language behavior in a circle of thalamus-cortical language areas. Left thalamic lesions can produce motor speech disturbances and aphasic disorders such as word-emission difficulties, and difficulties with comprehension (Jonas 1982). Moreover, the effects on speech production and verbal memory were evoked from the same general area of the thalamus that produced the language deficits, which raised the possibility that the thalamus is involved in coordinating the cognitive and motoric aspects of language production (Johnson and Ojemann 2000). Thus, the bilateral THA is crucial for language production and comprehension. Our study suggested that reduced bilateral THA volume may be a neural biomarker for PSA.

The activity of the right-sided precuneus are increased after training in aphasic patients those who with good naming recovery (Menke et al. 2009). Price et al. concluded that

activation in the PCUN is associated with the comparison of comprehensible and incomprehensible sentences (Price 2010). Furthermore, the PCUN was engaged in semantic processing (Binder et al. 2009). Both PCUN and IPL are included in the default mode network (DMN) (Broyd et al. 2009), which may be relevant for semantic processing (Xu et al. 2016). The precentral gyrus is a motor speech region that is influenced by nonfluent variants of primary progressive aphasia. In addition, some studies suggested that activation in the precentral gyrus may be related to phonological or phonetic encoding and execution of complex articulatory processing in language production (Dronkers 1996; Wise et al. 1999; Braun et al. 2001). The right postcentral gyrus is involved in representing action and object information, and these cognitive processes are affected by prior experience (Oliver et al. 2009). Therefore, we suggested that these increased connectivities may be indicative of a compensatory mechanism for language processing in aphasia.

This study has several methodological limitations. First, the sample size was relatively small, introducing difficulty in obtaining substantial evidence for abnormal local synchronization in aphasia. Second, the healthy subjects were not tested with ABC for language performance. Third, multiple comparisons for correlations between iFC values and clinical characteristics were not corrected. Further longitudinal work in larger samples is required to deeply explore the pathophysiological mechanisms of aphasia.

Conclusions

We found increased GMV in the right STG, IPL/SMG, and left MOG; and decreased GMV in the right CAU and bilateral THA. We suggest that increased gray matter in the right STG, IPL/SMG, and left MOG is conducive to compensating language processing in aphasia. Patients with PSA showed increased connectivity between the right PCUN, right IPL/SMG, and bilateral THA, which indicates that the right PCUN is an essential hub of language networks. In addition, we found decreased connectivity between the left MOG and other language regions. The FC values between the left MOG and the left ORBmid were positively correlated with the performance quotient from the ABC test in aphasic patients, suggesting that the left MOG may play a vital role in language processing. Our study provided evidence for the aberrances of FC between the DMN and bilateral THA in PSA patients. Changes in GMV and the associated remote iFC network can provide valuable information to enhance our understanding of the pathophysiological mechanisms of aphasia.

Acknowledgements We thank the radiologist Ying Liu (Y.L.) from the Hospital of Fuzhou for manually tracing the outline of the lesion.

This work was supported by the 863 project (2015AA020505), Natural Science Foundation of China (61533006 and 81471653), China Postdoctoral Science Foundation (2013M532229), Fundamental Research Funds for the Central Universities (ZYGX2013Z004), Sichuan provincial health and family planning commission research project (16PJ051), and the project of the Science and Technology Department in Sichuan province (2017JY0094).

Author Contributions DY, WL, and HC designed the study. MY, PY, YF and JL contributed to data collection. MY, PY, YF and JL contributed to data analysis, data interpretation, and manuscript preparation. All authors read and approved the final manuscript.

References

- Abdullaev YG, Bechtereva NP, Melnichuk KV (1998) Neuronal activity of human caudate nucleus and prefrontal cortex in cognitive tasks. *Behav Brain Res* 97:159–177
- Agosta F, Galantucci S, Valsasina P, Canu E, Meani A, Marcone A et al (2014) Disrupted brain connectome in semantic variant of primary progressive aphasia. *Neurobiol Aging* 35:2646–2655
- Ashburner J, Friston KJ (2000) Voxel-based morphometry—the methods. *Neuroimage* 11:805–821
- Ashizuka A, Mima T, Sawamoto N, Aso T, Oishi N, Sugihara G et al (2015) Functional relevance of the precuneus in verbal politeness. *Neurosci Res* 91:48–56
- Berthier ML (2005) Poststroke aphasia: epidemiology, pathophysiology and treatment. *Drugs Aging* 22:163–182
- Binder JR, Desai RH, Graves WW, Conant LL (2009) Where is the semantic system? A critical review and meta-analysis of 120 functional neuroimaging studies. *Cereb Cortex* 19:2767–2796
- Braun AR, Guillemin A, Hosey L, Varga M (2001) The neural organization of discourse—an (H₂O)-O-15-PET study of narrative production in English and American sign language. *Brain* 124:2028–2044
- Brett M, Leff AP, Rorden C, Ashburner J (2001) Spatial normalization of brain images with focal lesions using cost function masking. *Neuroimage* 14:486–500
- Broyd SJ, Demanuele C, Debener S, Helps SK, James CJ, Sonuga-Barke EJS (2009) Default-mode brain dysfunction in mental disorders: a systematic review. *Neurosci Biobehav Rev* 33:279–296
- Cavanna AE, Trimble MR (2006) The precuneus: a review of its functional anatomy and behavioural correlates. *Brain* 129:564–583
- Chao-Gan Y, Yu-Feng Z (2010) DPARSF: a MATLAB toolbox for “pipeline” data analysis of resting-state fmRI. *Front Syst Neurosci* 4:13–13
- Charney JZ (1981) Aphasia and associated disorders: taxonomy, localization, and recovery. *JAMA* 245:78
- Chou T-L, Booth JR, Bitan T, Burman DD, Bigio JD, Cone NE et al (2006a) Developmental and skill effects on the neural correlates of semantic processing to visually presented words. *Hum Brain Mapp* 27:915–924
- Chou TL, Booth JR, Burman DD, Bitan T, Bigio JD, Lu D et al (2006b) Developmental changes in the neural correlates of semantic processing. *Neuroimage* 29:1141–1149
- Crosson B, Benefield H, Cato MA, Sadek JR, Moore AB, Wierenga CE et al (2003) Left and right basal ganglia and frontal activity during language generation: contributions to lexical, semantic, and phonological processes. *J Int Neuropsychol Soc* 9:1061–1077
- Cuadra MB, Cammoun L, Butz T, Cuisenaire O, Thiran JP (2005) Comparison and validation of tissue modelization and statistical classification methods in T1-weighted MR brain images. *IEEE Trans Med Imaging* 24:1548–1565

- Dong JW, Brennan NMP, Izzo G, Peck KK, Holodny AI (2016) fMRI activation in the middle frontal gyrus as an indicator of hemispheric dominance for language in brain tumor patients: a comparison with Broca's area. *Neuroradiology* 58:513–520
- Dronkers NF (1996) A new brain region for coordinating speech articulation. *Nature* 384:159–161
- Dronkers NF, Wilkins DP, Van Valin RD Jr, Redfern BB, Jaeger JJ (2004) Lesion analysis of the brain areas involved in language comprehension. *Cognition* 92:145–177
- Ellis C, Simpson AN, Bonilha H, Mauldin PD, Simpson KN (2012) The one-year attributable cost of poststroke aphasia. *Stroke* 43:1429–1431
- Fox MD, Snyder AZ, Vincent JL, Corbetta M, Van Essen DC, Raichle ME (2005) The human brain is intrinsically organized into dynamic, anticorrelated functional networks. *Proc Natl Acad Sci USA* 102:9673–9678
- Fridriksson J, Richardson JD, Fillmore P, Cai B (2012) Left hemisphere plasticity and aphasia recovery. *Neuroimage* 60:854–863
- Gao SR, Chu YF, Shi S, Peng Q, Dai SD, Wang YMH (1992) A standardization research of the aphasia battery of Chinese. *Chin Mental Health J* 6:125–128
- Geva S, Baron JC, Jones PS, Price CJ, Warburton EA (2012) A comparison of VLSM and VBM in a cohort of patients with post-stroke aphasia. *Neuroimage Clin* 1:37–47
- Ghosh S, Basu A, Kumaran SS, Khushu S (2010) Functional mapping of language networks in the normal brain using a word-association task. *Indian J Radiol Imaging* 20:182–187
- Girbau-Massana D, Garcia-Marti G, Marti-Bonmati L, Schwartz RG (2014) Gray-white matter and cerebrospinal fluid volume differences in children with specific language impairment and/or reading disability. *Neuropsychologia* 56:90–100
- Good CD, Johnsrude IS, Ashburner J, Henson RNA, Friston KJ, Frackowiak RSJ (2001) A voxel-based morphometric study of ageing in 465 normal adult human brains. *Neuroimage* 14:21–36
- Greicius MD, Supekar K, Menon V, Dougherty RF (2009) Resting-state functional connectivity reflects structural connectivity in the default mode network. *Cereb Cortex* 19:72–78
- Hagmann P, Sporns O, Madan N, Cammoun L, Pienaar R, Wedeen VJ et al (2010) White matter maturation reshapes structural connectivity in the late developing human brain. *Proc Natl Acad Sci USA* 107:19067–19072
- Hartwigsen G, Baumgaertner A, Price CJ, Koehnke M, Ulmer S, Siebner HR (2010) Phonological decisions require both the left and right supramarginal gyri. *Proc Natl Acad Sci USA* 107:16494–16499
- Honey CJ, Sporns O, Cammoun L, Gigandet X, Thiran JP, Meuli R et al (2009) Predicting human resting-state functional connectivity from structural connectivity. *Proc Natl Acad Sci USA* 106:2035–2040
- Ji GJ, Zhang Z, Xu Q, Zang YF, Liao W, Lu G (2014) Generalized tonic-clonic seizures: aberrant interhemispheric functional and anatomical connectivity. *Radiology* 271:839–847
- Johnson MD, Ojemann GA (2000) The role of the human thalamus in language and memory: evidence from electrophysiological studies. *Brain Cogn* 42:218–230
- Jonas S (1982) The thalamus and aphasia, including transcortical aphasia: a review. *J Commun Disord* 15:31–41
- Just MA, Cherkassky VL, Keller TA, Minshew NJ (2004) Cortical activation and synchronization during sentence comprehension in high-functioning autism: evidence of underconnectivity. *Brain* 127:1811–1821
- Kana RK, Keller TA, Cherkassky VL, Minshew NJ, Just MA (2006) Sentence comprehension in autism: thinking in pictures with decreased functional connectivity. *Brain* 129:2484–2493
- Kochunov P, Thompson PM, Lancaster JL, Bartzokis G, Smith S, Coyle T et al (2007) Relationship between white matter fractional anisotropy and other indices of cerebral health in normal aging: tract-based spatial statistics study of aging. *Neuroimage* 35:478–487
- Liao W, Xu Q, Mantini D, Ding J, Machado-de-Sousa JP, Hallak JE et al (2011a) Altered gray matter morphometry and resting-state functional and structural connectivity in social anxiety disorder. *Brain Res* 1388:167–177
- Liao W, Zhang Z, Pan Z, Mantini D, Ding J, Duan X et al (2011b) Default mode network abnormalities in mesial temporal lobe epilepsy: a study combining fMRI and DTI. *Hum Brain Mapp* 32:883–895
- Liao W, Yu Y, Miao HH, Feng YX, Ji GJ, Feng JH (2017) Inter-hemispheric intrinsic connectivity as a neuromarker for the diagnosis of boys with Tourette syndrome. *Mol Neurobiol* 54:2781–2789
- Liu L, Luo X-G, Dy C-L, Ren Y, Feng Y, Yu H-M et al (2015) Characteristics of language impairment in Parkinson's disease and its influencing factors. *Transl Neurodegener* 4:2–2
- Long Z, Xu Q, Miao HH, Yu Y, Ding MP, Chen H et al (2017) Thalamo-cortical dysconnectivity in paroxysmal kinesigenic dyskinesia: Combining functional magnetic resonance imaging and diffusion tensor imaging. *Mov Disord* 32:592–600
- Lu J, Wu J, Yao C, Zhuang D, Qiu T, Hu X et al (2013) Awake language mapping and 3-Tesla intraoperative MRI-guided volumetric resection for gliomas in language areas. *J Clin Neurosci* 20:1280–1287
- Martensson F, Roll M, Lindgren M, Apt P, Horne M (2014) Sensory-specific anomia following left occipital lesions: data from free oral descriptions of concrete word meanings. *Neurocase* 20:192–207
- Menke R, Meinzer M, Kugel H, Deppe M, Baumgaertner A, Schiffbauer H et al (2009) Imaging short- and long-term training success in chronic aphasia. *BMC Neurosci* 10:118
- Musso M, Weiller C, Kiebel S, Muller SP, Bulau P, Rijntjes M (1999) Training-induced brain plasticity in aphasia. *Brain* 122:1781–1790
- Nair VA, Young BM, La C, Reiter P, Nadkarni TN, Song J et al (2015) Functional connectivity changes in the language network during stroke recovery. *Ann Clin Transl Neurol* 2:185–195
- Ogar JM, Baldo JV, Wilson SM, Brambati SM, Miller BL, Dronkers NF et al (2011) Semantic dementia and persisting Wernicke's aphasia: Linguistic and anatomical profiles. *Brain Lang* 117:28–33
- Oliver RT, Geiger EJ, Lewandowski BC, Thompson-Schill SL (2009) Remembrance of things touched: How sensorimotor experience affects the neural instantiation of object form. *Neuropsychologia* 47:239–247
- Power JD, Barnes KA, Snyder AZ, Schlaggar BL, Petersen SE (2012) Spurious but systematic correlations in functional connectivity MRI networks arise from subject motion. *Neuroimage* 59:2142–2154
- Price CJ (2010) The anatomy of language: a review of 100 fMRI studies published in 2009. *Ann NY Acad Sci* 1191:62–88
- Price CJ, Devlin JT (2003) The myth of the visual word form area. *Neuroimage* 19:473–481
- Radulescu E, Minati L, Ganeshan B, Harrison NA, Gray MA, Beacher FDCC et al (2013) Abnormalities in fronto-striatal connectivity within language networks relate to differences in grey-matter heterogeneity in Asperger syndrome. *Neuroimage Clin* 2:716–726
- Raposo A, Moss HE, Stamatakis EA, Tyler LK (2006) Repetition suppression and semantic enhancement: An investigation of the neural correlates of priming. *Neuropsychologia* 44:2284–2295
- Sakai KL, Nauchi A, Tatsuno Y, Hirano K, Muraishi Y, Kimura M et al (2009) Distinct roles of left inferior frontal regions that explain individual differences in second language acquisition. *Hum Brain Mapp* 30:2440–2452
- Sims JA, Kapse K, Glynn P, Sandberg C, Tripodis Y, Kiran S (2016) The relationships between the amount of spared tissue, percent

- signal change, and accuracy in semantic processing in aphasia. *Neuropsychologia* 84:113–126
- Sollmann N, Tanigawa N, Ringel F, Zimmer C, Meyer B, Krieg SM (2014) Language and its right-hemispheric distribution in healthy brains: an investigation by repetitive transcranial magnetic stimulation. *Neuroimage* 102:776–788
- Stebbins GT, Nyenhuis DL, Wang C, Cox JL, Freels S, Bangen K et al (2008) Gray matter atrophy in patients with ischemic stroke with cognitive impairment. *Stroke* 39:785–793
- Turken AU, Dronkers NF (2011) The neural architecture of the language comprehension network: converging evidence from lesion and connectivity analyses. *Front Syst Neurosci* 5:1–1
- van Hees S, McMahon K, Angwin A, de Zubicaray G, Read S, Copland DA (2014a) Changes in white matter connectivity following therapy for anomia post stroke. *Neurorehabil Neural Repair* 28:325–334
- van Hees S, McMahon K, Angwin A, de Zubicaray G, Read S, Copland DA (2014b) A functional MRI study of the relationship between naming treatment outcomes and resting state functional connectivity in post-stroke aphasia. *Hum Brain Mapp* 35:3919–3931
- Wang X, Wang M, Wang W, Liu H, Tao J, Yang C et al (2014) Resting state brain default network in patients with motor aphasia resulting from cerebral infarction. *Chin Sci Bull* 59:4069–4076
- Wise RJS, Greene J, Buchel C, Scott SK (1999) Brain regions involved in articulation. *The Lancet* 353:1057–1061
- Xu Y, Lin Q, Han Z, He Y, Bi Y (2016) Intrinsic functional network architecture of human semantic processing: modules and hubs. *Neuroimage* 132:542–555
- Yang M, Li J, Li Y, Li R, Pang Y, Yao D et al (2016a) Altered intrinsic regional activity and interregional functional connectivity in post-stroke aphasia. *Sci Rep* 6:24803
- Yang M, Li J, Yao D, Chen H (2016b) Disrupted intrinsic local synchronization in poststroke aphasia. *Medicine* 95:e3101
- Yang M, Li Y, Li J, Yao D, Liao W, Chen H (2017) Beyond the arcuate fasciculus: damage to ventral and dorsal language pathways in aphasia. *Brain Topogr* 30:249–256
- Zeng LL, Wang D, Fox MD, Sabuncu M, Hu D, Ge M et al (2014) Neurobiological basis of head motion in brain imaging. *Proc Natl Acad Sci USA* 111:6058–6062
- Zhang Z, Liao W, Chen H, Mantini D, Ding JR, Xu Q et al (2011) Altered functional-structural coupling of large-scale brain networks in idiopathic generalized epilepsy. *Brain* 134:2912–2928
- Zhu D, Chang J, Freeman S, Tan Z, Xiao J, Gao Y et al (2014) Changes of functional connectivity in the left frontoparietal network following aphasic stroke. *Front Behav Neurosci* 8:167